

Heavy ion transfer reactions: ongoing and future experiments performed with large acceptance magnetic spectrometers

L. Corradi^{1,a}

¹ INFN - Laboratori Nazionali di Legnaro - Viale dell'Università 2, 35020, Legnaro (Padova) - Italy

Abstract.

The advent of the last generation large solid angle magnetic spectrometers, coupled to large gamma arrays, allowed to perform gamma-particle coincidences for nuclei moderately far from stability, especially in the neutron-rich region. Via transfer of multiple pairs valuable information on nucleon-nucleon correlations can also be derived, especially from measurements performed below the Coulomb barrier. There is growing interest in the study of the properties of the heavy binary partner, in the Pb and in the actinides regions, crucial also for astrophysics.

1 Introduction

Traditionally, via multinucleon transfer reactions at Coulomb barrier energies one can investigate nucleon-nucleon correlation in nuclei, the transition from the quasi-elastic to the deep-inelastic regime and channel coupling effects in sub-barrier fusion reactions [1]. This mechanism, where many nucleons are transferred and where nuclear structure still plays a significant role in the dynamics, since one decade is at a focus of important experimental and theoretical advances. The advent of the last generation large solid angle magnetic spectrometers [2–5] coupled to large gamma arrays [6–8] allowed to perform gamma-particle coincidences, thus studying at the same time reaction mechanism and nuclear structure for nuclei produced via nucleon transfer or deep-inelastic reactions, especially in the neutron-rich region. Ongoing studies are of primary importance for reactions to be done with radioactive ion beams [9, 10] where multinucleon transfer has been shown to be a competitive tool for the study of neutron-rich nuclei, at least for certain mass regions. In the following, selected examples of studied reactions will be presented, with some emphasis on recent experiments performed at sub-barrier energies and on future investigations in the heavy mass regions [11].

2 Some properties of quasi elastic processes

In Fig. 1 is shown a representative example of the mass and charge distribution of transfer products in the $^{40}\text{Ca}+^{208}\text{Pb}$ system [12]. The bombarding energy is close to the Coulomb barrier and the yield, measured at the grazing angle, reflects some of the main characteristics

of quasi-elastic processes [13]. The two dash-dotted lines correspond to pure neutron pick-up and pure proton stripping channels, while the full line represents the charge equilibration, namely the location of the N/Z ratio of the compound nucleus. One sees that most nuclei are located on the left side of the charge equilibration line, indicating the dominance of a direct mechanism in the population of different fragments. Notice also that for the massive proton transfer channels the isotopic distributions drift towards lower masses, evidencing that these distributions are affected by secondary processes [12, 14]. In Fig. 2 we

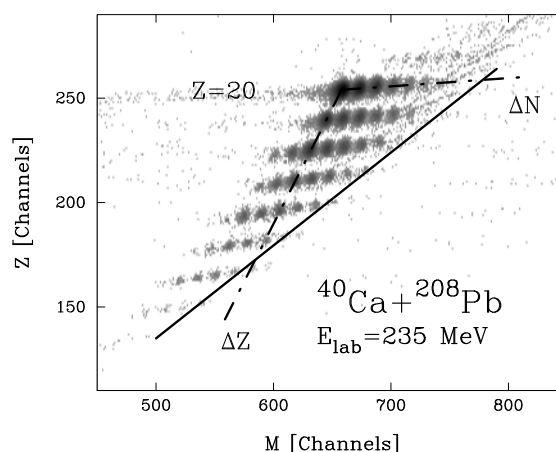


Figure 1. Mass-charge distributions of transfer products in the $^{40}\text{Ca}+^{208}\text{Pb}$ reaction at $E_{\text{lab}} = 235$ MeV obtained at the grazing angle, $\theta_{\text{lab}} = 84^\circ$. The dash-dotted lines correspond to the pure proton stripping (ΔZ) and to the pure neutron pick-up (ΔN) channels, crossing at $Z=20$ and $A=40$. The full line shows the charge equilibration, namely, the N/Z ratio of the compound nucleus

^ae-mail: corradi@lnl.infn.it

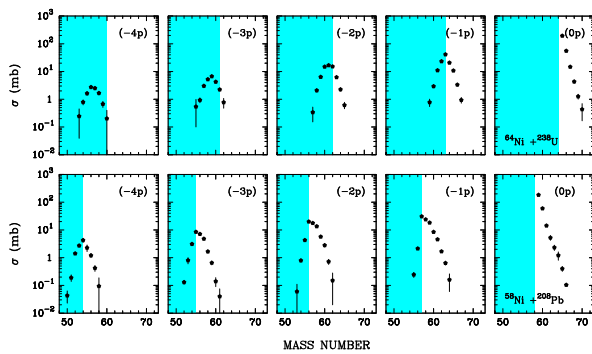


Figure 2. Isotopic distributions for the transfer channels up to the stripping of four protons are shown for the reaction $^{64}\text{Ni} + ^{238}\text{U}$ at 390 MeV bombarding energy (top) and for the reaction $^{58}\text{Ni} + ^{208}\text{Pb}$ at 328 MeV bombarding energy (bottom). The shaded regions mark the transition from neutron stripping to neutron pick-up

plot the isotopic distribution of the different charges populated in the $^{64}\text{Ni} + ^{238}\text{U}$ and $^{58}\text{Ni} + ^{208}\text{Pb}$ reactions [14, 15]. One observes that the strongest channels are those corresponding to the neutron pick-up and proton stripping processes, as the optimum Q -value rule suggests. It is only for charges far from the entrance channel that one observes sizeable contributions that seems to derive from the stripping of neutrons, this is particularly evident for the collision with uranium where the isotopic distributions peak at masses lighter than the pure proton stripping channels. Indeed, these channels can be populated via other complex processes like evaporation, deep inelastic or fission. The simple findings depicted in Figs. 1 and 2 have been demonstrated in almost all measured systems and holds for most of the projectile-target combinations available with stable beams. By employing neutron rich beams also proton pick-up and neutron stripping channels open up [16], implying important aspects that will be discussed in Sect. 5.

3 Cross sections

One of the major achievements of significant instrumental value was the possibility to extract, within certain limits, absolute cross sections with large acceptance magnetic spectrometers. One has to keep in mind that with these devices it becomes unfeasible to use complex magnetic elements to correct for the ion optical aberrations, thus a simplified magnetic element configuration and the concept of trajectory reconstruction has been adopted. In order to obtain the differential cross sections the response function of the spectrometer, which depends in a complex way on the entrance angles and momenta of the reaction products, has been studied and devoted algorithms have been developed [17]. The extracted transmission factors are then applied as a correction to the experimental differential cross sections. As an example Fig. 3 displays

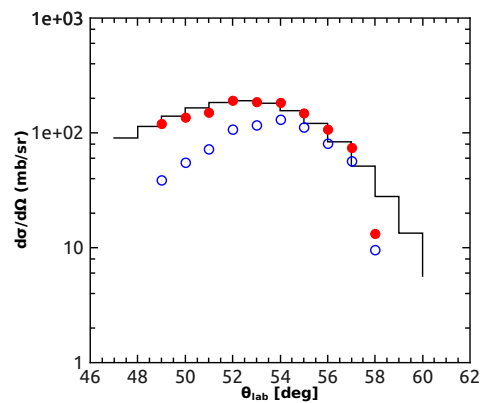


Figure 3. Angular distribution for ^{41}Ar in the $^{40}\text{Ar} + ^{208}\text{Pb}$ reaction at $E_{lab}=255$ MeV. PRISMA was positioned at the grazing angle $\theta_{lab}=54^\circ$. Empty symbols are the pure experimental results and full symbols are the experimental results after the correction factor was applied. The solid line is the differential cross section obtained with the GRAZING code

the angular distribution of ^{41}Ar in the $^{40}\text{Ar} + ^{208}\text{Pb}$ reaction [18], where empty circles are the data directly extracted from experiment, while the full circles are those corrected for the transmission of the spectrometer. In addition, the GRAZING [19–21] calculation (see below) is added as a histogram. One sees the good agreement with the theoretical calculations. These calculations, in particular for one-particle transfer channels, reproduced a wealth of experimental data [1] and can be taken as a good reference. As expected, major corrections (and presently the main source of systematic errors in extracting final absolute values) are needed when approaching the edge of the angular acceptance. The size of the corrections depends also strongly on the kinetic energy of the transported ions and should become progressively more relevant as one moves from low bombarding energies (narrow Q values) to cases where deep inelastic components set-in. The successful application of the correction method for a system measured at a bombarding energy ≈ 2.5 the Coulomb barrier and at quite forward angles has been shown in the case of the $^{48}\text{Ca} + ^{64}\text{Ni}$ reaction [17, 22].

With PRISMA, total yield distributions for multineutron and multiproton transfer channels have been extracted in various systems close to the Coulomb barrier, for instance in the reactions $^{40}\text{Ca} + ^{96}\text{Zr}$ [3], $^{90}\text{Zr} + ^{208}\text{Pb}$ [3, 23] and $^{40}\text{Ar} + ^{208}\text{Pb}$ [18]. The full efficiency of the spectrometer can be appreciated from Fig. 4 which shows the total angle and Q -value integrated yields for multineutron and multiproton transfer channels populated in the reaction $^{90}\text{Zr} + ^{208}\text{Pb}$. Sensitivity was sufficient to observe the transfer of very large number of proton stripping channels.

In the selected cases, the chosen projectiles and targets are closed shell or near-closed shell nuclei and therefore ideal candidates for a quantitative comparison with theoretical models [20, 21]. Figure 5 shows as an example the experimental total cross sections for the pure neutron pick-

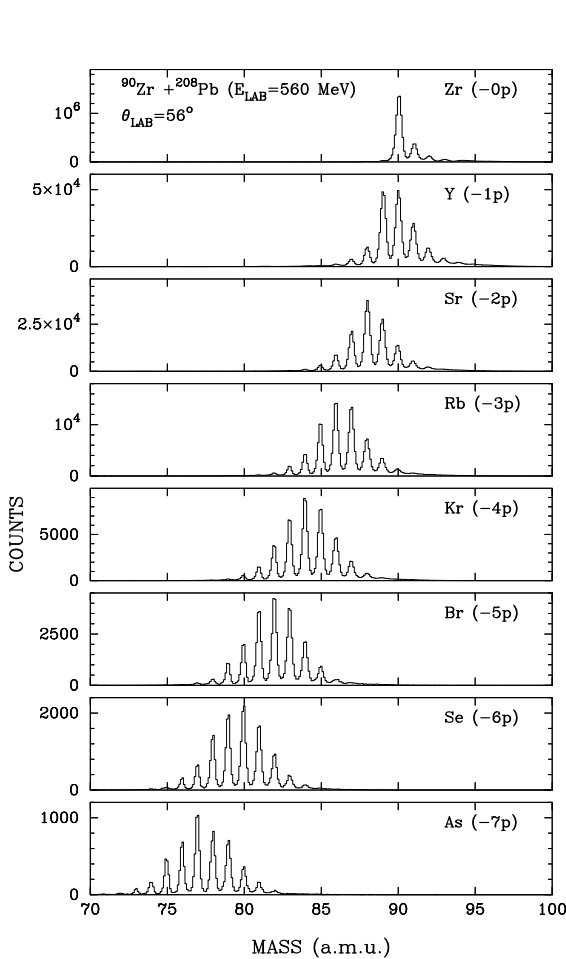


Figure 4. Mass distributions of transfer products for different Z in the reaction $^{90}\text{Zr} + ^{208}\text{Pb}$ at $E_{\text{lab}} = 560$ MeV. The displayed mass distributions stop at seven proton stripping ($-7p$) channels only to limit the length of the figure

up channels in $^{90}\text{Zr} + ^{208}\text{Pb}$ and $^{40}\text{Ca} + ^{96}\text{Zr}$ systems and the channels involving the one proton stripping in $^{40}\text{Ca} + ^{96}\text{Zr}$ [3]. The data are compared with calculations performed with the semiclassical code GRAZING [19]. This model calculates the evolution of the reaction by taking into account, besides the relative motion variables, the intrinsic degrees of freedom of projectile and target. These are the surface degrees of freedom and particle transfer. The exchange of many nucleons proceeds via a multi-step mechanism of single nucleons (both, protons and neutrons, via stripping, and pick-up processes). As the relative motion of the system is calculated in a nuclear plus Coulomb field, the precise definition of the potential is crucial for the good description of the reaction dynamics. This model has been successfully applied in the description of multi-nucleon transfer reactions [1] and can reproduce the near-barrier fusion excitation functions [24] and extracted barrier distributions [25]. One can mention that other models have been recently employed to compute multinucleon transfer cross sections, based on Langevin-type dynamical equations of motion [26], di-nuclear system models [27],

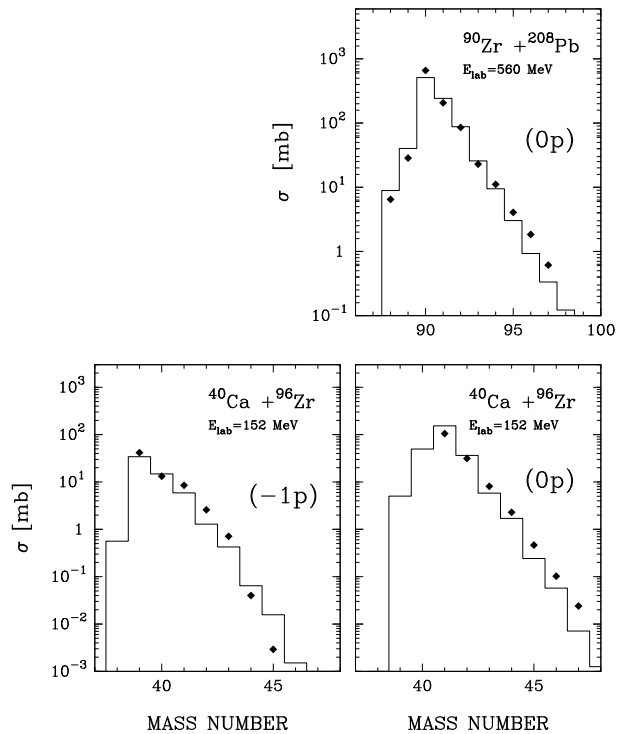


Figure 5. Top : Total cross sections for pure neutron pick-up channels in the $^{90}\text{Zr} + ^{208}\text{Pb}$ reaction. Bottom: Total cross sections for pure neutron pick-up (right panel) and one-proton stripping (left panel) channels in the $^{40}\text{Ca} + ^{96}\text{Zr}$ reaction. The points are the experimental data and the histograms are the GRAZING code calculations

Hartree-Fock-Bogoliubov theory [28] and on a fully microscopic framework of the time-dependent Hartree-Fock theory and its extensions [29–34].

Looking at the experimental data of Fig. 5 one finds that the cross sections for the neutron pick-up drop by almost a constant factor for each transferred neutron, as an independent particle mechanism would suggest. The comparison with calculations supports this idea; one notices a remarkable agreement both on the neutron pick-up as well as on the neutron stripping side. One can mention that the pure proton cross sections behave differently, with the population of the ($-2p$) channel as strong as the ($-1p$) channel [12]. This suggests the contribution of processes involving the transfer of proton pairs in addition to the successive transfer of single protons. As discussed before, one also observes that as more protons are transferred the average mass shifts to lower neutron number. This is mostly attributed to the effect of neutron evaporation from the primary fragments. This effect of neutron evaporation is indirectly visible from the analysis of Refs. [12, 14] and has been also directly seen by means of γ -particle coincidences, as presented in the next Section.

4 Energy loss effects

The Z and A identification capability and the large detection efficiency of PRISMA allow to follow the evolution

of the reaction from the quasi elastic to the deep inelastic regime. In Figs. 6 and 7 are shown the mass distributions and associated Total Kinetic Energy Loss (TKEL) spectra of representative transfer channels for the $^{90}\text{Zr}+^{208}\text{Pb}$ reaction. One can clearly follow the evolution pattern as function of the number of transferred neutrons and protons. In the case of pure neutron transfers one sees a quasi-elastic peak and an increasing strength of large energy loss components when adding neutrons. When protons are involved one observes a faster growth of large TKEL components, and beyond three-proton stripping the TKEL distributions have almost similar shapes. We remind that one detects secondary fragments and that the TKEL spectra are constructed assuming binary reactions, so the shapes may be somewhat modified with respect to the (unreconstructed) primary fragments. Looking at the mass distributions, for

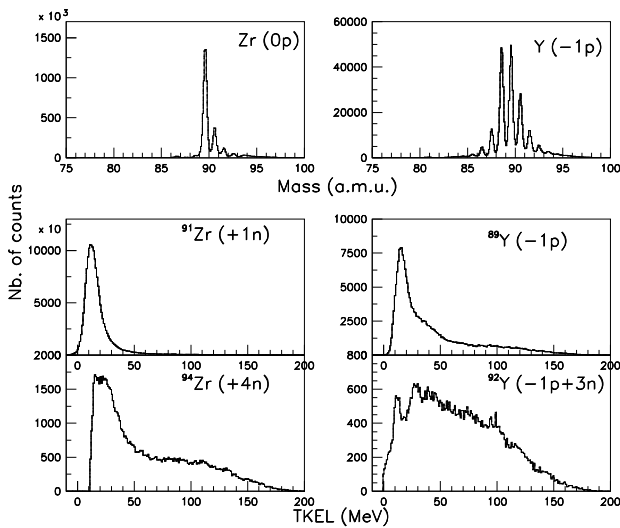


Figure 6. Mass (top panels) and TKEL (middle and bottom panels) spectra obtained in the reaction $^{90}\text{Zr}+^{208}\text{Pb}$ for the indicated transfer channels. $(0p)$ and $(-1p)$ in the mass spectra refer to Zr and Y isotopes, respectively

few nucleon transfer one has a situation typical of quasi-elastic processes, well defined by the Q values, while for many nucleon transfer the shape of the mass distribution is much broader (more Gaussian-like). The yields of specific proton transfer channels $(-xp \pm yn)$ are distributed over more masses and the pure proton stripping channels become less favourite as more protons are transferred, with the centroids of the mass distributions shifting to lower values. This behaviour is strongly connected with the effect of nucleon evaporation from the primary fragments, in turn associated with large energy losses. The importance of neutron evaporation in the modification of the final yield distribution can be directly seen via γ -particle coincidences. Gating on a specific Z and A (light partner) identified with a spectrometer, the velocity vector of the undetected heavy partner can be evaluated and applied

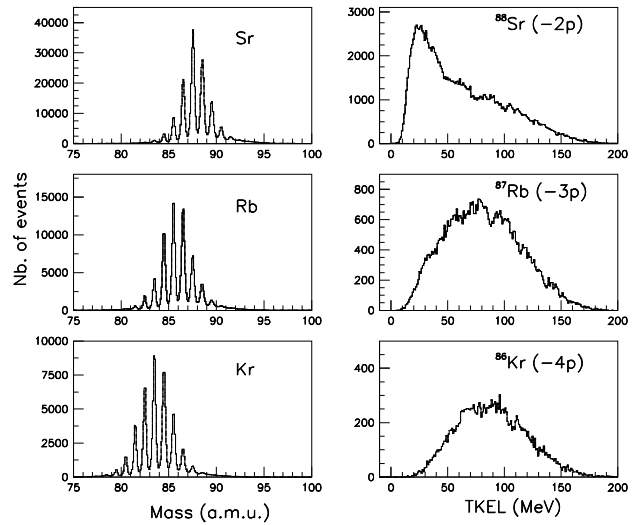


Figure 7. Mass and TKEL spectra obtained in the reaction $^{90}\text{Zr}+^{208}\text{Pb}$ for the indicated proton stripping transfer channels

for the Doppler correction of its corresponding γ rays. In those spectra not only the γ rays belonging to the primary binary partner are present, but also the ones of the nuclei produced after evaporation takes place. An example is given in Fig. 8 for the $(-2p)$, $(-2p+1n)$ and $(-2p+2n)$ channels populated in the $^{40}\text{Ca}+^{96}\text{Zr}$ reaction [3].

5 Population of the n-rich heavy region

5.1 Light fragments

Based on the present understanding of the transfer mechanism, at least for inclusive data, different experiments have been performed in the last years using PRISMA [2, 3] in combination with the CLARA [6] and AGATA-demonstrator [8] γ array. By exploiting the large efficiency and resolution of PRISMA, one could detect neutron-rich nuclei in the mass region from Ne to Xe and get information on the properties of their lowest energy levels (see e.g. Refs. [35–39] and references therein). In many cases the new gamma transitions have been uniquely attributed to the specific isotopes identified by the spectrometer via particle-gamma coincidences. A wide experimental program of nuclear spectroscopy measurements has been also carried out with the EXOGAM γ array [7] coupled to the VAMOS [4] magnetic spectrometer, exploiting in particular the ^{238}U beams provided in GANIL [40–43]. Measurements on spectroscopic factors in light ion induced reactions of Ne and O radioactive beams have been also obtained, adding important new information on the behaviour of shell gaps toward the neutron rich region [44, 45].

A novel powerful technique has been successfully developed to measure lifetimes of excited states populated in binary reactions, by exploiting the different intensities of the Doppler shifted γ rays emitted before and after

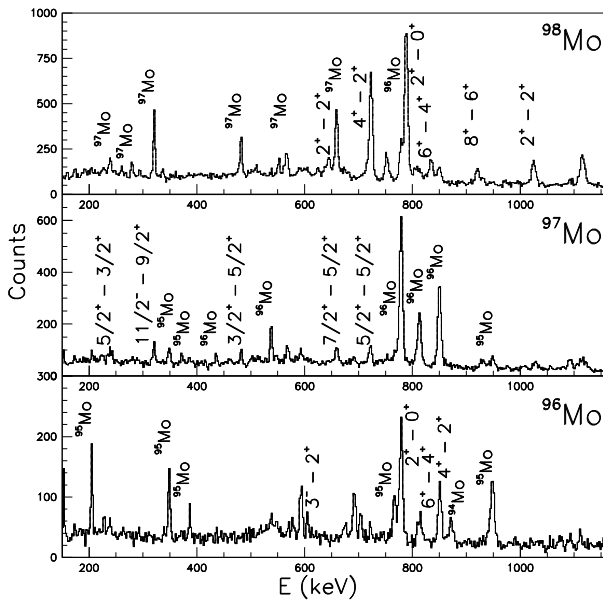


Figure 8. γ spectra obtained in the reaction $^{40}\text{Ca}+^{96}\text{Zr}$, Doppler corrected for the heavy fragments. The main labels ^{98}Mo , ^{97}Mo and ^{96}Mo in each frame indicate the primary heavy fragments, populated via the $(-2p)$, $(-2p+1n)$ and $(-2p+2n)$ channels, respectively, and whose spectra correspond to ^{38}Ar , ^{39}Ar and ^{40}Ar tagged with PRISMA

a degrader placed close to the target [46, 47]. Lifetime measurements have been performed for a variety of nuclei, providing new information on electromagnetic transition probabilities, to be compared with large scale shell model calculations. By using multinucleon transfer reactions it was possible to investigate chains of isotopes populated, at once, in the same reaction [48–50]. Thus, poorly known (neutron rich) isotopes could be more easily compared with better known ones, making the attribution of level properties more reliable when coincidences between particles and single gamma are available. Here, in the recognition of the character of the lowest populated states the main characteristic of the multinucleon transfer reaction mechanism helps in the attribution of the spins of the new transitions. Being the transfer of few nucleons a direct mechanism, strong population of states with the single-particle character has been observed for instance in the $^{40}\text{Ar}+^{208}\text{Pb}$ reaction [48]. In addition, the states whose structure can be connected with the vibration/rotation quanta are expected to be strongly excited in these heavy-ion-induced transfers. In fact it is through the excitation of the elementary modes, surface vibrations and single particles, that energy and angular momentum are transferred from the relative motion to these intrinsic degrees of freedom and that mass and charge are exchanged among the two partners of the collision. The transfer mechanism provides also a tool to build-up a high degree of alignment. On this basis, exploiting the granularity of

the γ arrays, measurements of γ -ray angular distributions and linear polarizations have been shown to be a powerful tool to determine the multipolarity and electromagnetic character of the transitions [51, 52].

5.2 Heavy fragments

Besides the “light” partner products, the “heavy” partners are presently receiving peculiar attention. In fact, certain regions of the nuclear chart, like that below ^{208}Pb or in the actinides, can be hardly accessed by fragmentation or fission reactions, and multinucleon transfer may be a suitable mechanism to approach those neutron rich areas. We remind, as an example, that nuclear properties of neutron rich nuclei around $N=126$ are relevant for the r -process, and play a critical role for theoretical predictions of the synthesis of the heaviest elements [26], for disentangling a variety of astrophysical scenarios [53, 54], and to study the competition between Gamow-Teller and First-Forbidden β transitions [54].

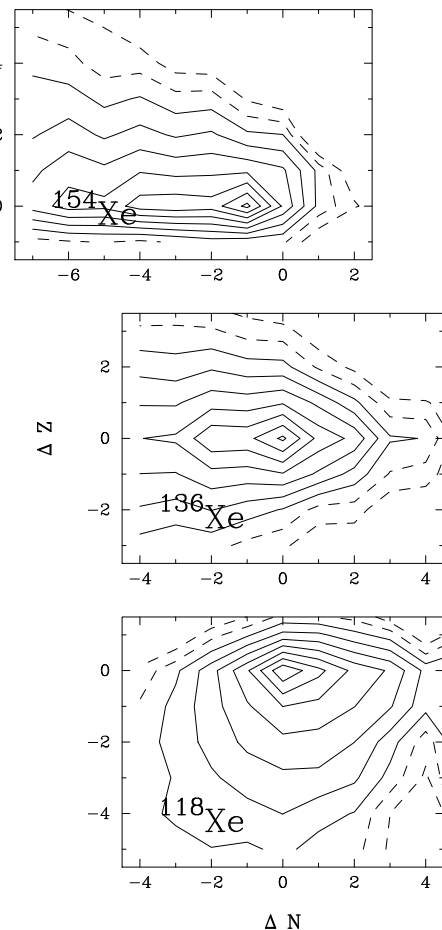


Figure 9. GRAZING code calculations for the production yields of multinucleon transfer reactions as a function of ΔN (number of transferred neutrons) and ΔZ (number of transferred protons). The results refer to the collision of Xe isotopes on ^{208}Pb at $E_{cm}=700$ MeV. The frames correspond to ^{118}Xe (bottom), ^{136}Xe (middle) and ^{154}Xe (top). Each two lines is one order of magnitude

To understand how one can approach the neutron rich heavy region, we have to keep in mind that transfer processes are governed by form factors and optimum Q -value considerations. With neutron poor projectiles on heavy targets only proton stripping and neutron pick-up channels are available, while with neutron rich projectiles also proton pick-up and neutron stripping channels open up [16]. This corresponds, for the heavy partner, to the population in the “south-east” direction, leading to the neutron rich heavy region. For the characteristic behaviour of the binding energy, the process is essentially governed by the lighter partner of the reaction. In Fig. 9 is shown an example of GRAZING calculations for the collision of different Xe beams on ^{208}Pb target. The figure indicates the change of population pattern from ^{118}Xe (neutron poor) to ^{154}Xe (neutron rich) isotopes. The calculated production yield is already corrected by neutron evaporation, which of course limits the final yield of neutron rich nuclei very far from stability.

This change of population pattern has been experimentally shown in different heavy ion reactions by directly detecting in Z and A the light partner products. In addition, as outlined before, via γ -particle coincidences, coincident “heavy” recoils have been identified via their associated γ rays. Along similar lines, an experiment has been very recently performed in the $^{136}\text{Xe}+^{198}\text{Pt}$ reaction [55], with the main purpose of studying the yield distribution of light and associated heavy transfer products. Integral experiments are being performed in Jyväskylä and Dubna to extract and study “off-line” nuclei in the Os region produced via deep inelastic processes in $^{136}\text{Xe}+^{208}\text{Pb}$. A project has been also launched by a KEK Japanese group to use deep inelastic reactions to produce, extract and identify heavy nuclei in the $N=126$ region [56].

Direct detection of the heavy products ($A\sim 150-200$) is notoriously very difficult. One has to keep in mind that the bombarding energy must be close to the Coulomb barrier as a compromise between having high primary cross sections and reasonable final (detected) yield after secondary processes occur. Due to the low ion kinetic energies, A and Z resolutions become worse. Significant progress can be made by using reactions in inverse kinematics, where ions are forward focused (high efficiency) and with high kinetic energy [57, 58]. Of course, at least with conventional spectrometers, care has to be taken in handling detector rates at forward angles.

The mechanism of fission deserve some comments, in particular transfer induced fission, affecting generally the heavy partner. From the point of view of γ spectroscopy, this turns out to be an efficient way to populate neutron rich nuclei. First experiments where fission products are selected in A and Z with a spectrometer and their associated γ rays are detected with large γ arrays have been already performed. For instance, the reaction $^{136}\text{Xe}+^{238}\text{U}$ [59] has been employed to measure the lowest energy levels of ^{96}Kr and study the evolution of quadrupole deformation in that region. The $^{238}\text{U}+^{12}\text{C}$ reaction [60] has been used to populate neutron rich nuclei in the mass range $A\sim 100-140$,

where properties of newly identified levels have been compared with large scale shell model calculations.

As said before, the competitive processes of evaporation and/or fission shift the final yield to lower mass values. Fission becomes of course more and more crucial in governing the decay process in the actinides and transactinides region [61]. It is therefore extremely important to get quantitative information on the final yield distributions and compare them with theoretical predictions. High resolution kinematic coincidences are expected to bring important information on these processes. As an example, in the $^{58}\text{Ni}+^{208}\text{Pb}$ measurement of Ref. [14] the relevance of transfer induced fission and how the experimental values can be quite well described by the same theory used to compare with the distributions of the light partner have been discussed.

6 Reactions at sub-barrier energies

At energies well below the Coulomb barrier, the interacting nuclei are only slightly influenced by the nuclear potential and Q values are restricted to few MeV for the open transfer channels. These conditions diminish the complexity of coupled channel calculations and quantitative information may be extracted on the nucleon-nucleon correlations [62–64]. In literature many data on transfer reactions have been represented via the transfer probability (P_{tr}) plotted as a function of the distance of closest approach (D) but quite contradictory conclusion have been extracted, since data have been mostly taken at energies above the Coulomb barrier.

The coming into operation of large acceptance magnetic spectrometers made it possible to perform measurements on multinucleon transfer reactions with good ion identification also at very low bombarding energies [58]. With this experimental advance we are now in condition to study the interplay between single and pair transfers far below the Coulomb barrier and thus to provide an answer on the origin of the enhancement reported for these reactions (cfr. e.g. Ref. [65] and references therein). In very recently measured systems one successfully demonstrated the powerful method of using PRISMA for such studies, exploiting its unique performance in terms of both resolution and efficiency. Making use of inverse kinematics, target recoils have been detected in multinucleon transfer reactions for the systems $^{96}\text{Zr}+^{40}\text{Ca}$ [58] and $^{116}\text{Sn}+^{60}\text{Ni}$ [66]. In both cases an excitation function at several bombarding energies has been obtained from the Coulomb barrier to 20-25% below, reaching about 15.5 fm of distance of closest approach.

Results of the measurement of the $^{96}\text{Zr}+^{40}\text{Ca}$ system (closed shell nuclei) are presented, together with the calculations, in Fig. 10 for $(+1n)$ and $(+2n)$ neutron transfer channels via transfer probabilities as a function of the distance of closest approach. A significant transfer yield could be detected at the level of 10^{-4} with respect to the elastic channel. To compute the inclusive one-neutron stripping cross section (full line) one calculated the transfer probability for a given single particle transition and one

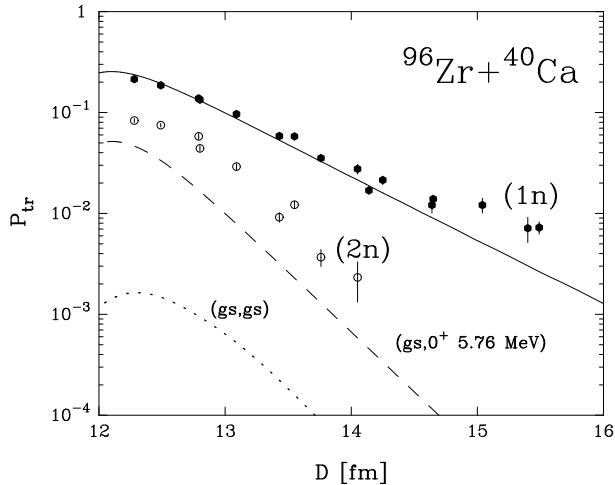


Figure 10. Points: Experimental transfer probabilities as a function of the distance of closest approach for (+1n) (full circles) and (+2n) (empty circles) for the $^{96}\text{Zr}+^{40}\text{Ca}$ system. Lines: Theoretical transfer probabilities for one and two particle transfer. The full line represents the inclusive transfer probability for one neutron transfer, the dotted line the ground-ground state transition for the two-neutron transfer and the dash line the transition to the first 0^+ excited state at ~ 5.8 MeV in ^{42}Ca

obtained the total transfer probability by summing over all possible transitions that can be constructed from the single particle states in projectile and target. One sees how calculations reproduce well the experimental data as well as the absolute values of the transfer probabilities for the one neutron channel. For the two-particle transfer one followed closely the formalism of Ref. [64]. We here just mention that the ground state wave function for the ^{94}Zr is obtained from a BCS calculation by adopting a state independent pairing interaction, while for the description of ^{42}Ca one diagonalized the total Hamiltonian with a model space containing only two-particle configuration coupled to 0^+ (i.e. transfer of a $J = 0^+$ pair). In Fig. 10 with a dotted line is shown the calculated probability for the ground-ground state transition. Clearly, this transition does not contribute to the total transfer strength in agreement with what was experimentally observed in the Q -value spectra. The predicted transfer probability for the transition to the 0^+ state at ~ 5.8 MeV in ^{42}Ca [67] is shown with a dashed line. It is apparent that the contribution of this transition is much larger than the ground state one. One presently ascribes the enhancement factor of ~ 3 to the fact that the two-nucleon transfer reaction does not populate only 0^+ states but it is much richer, so that more complicated two-particle correlations have to be taken into account.

At variance with the $^{96}\text{Zr}+^{40}\text{Ca}$ system (closed shell), in the very recently studied $^{116}\text{Sn}+^{60}\text{Ni}$ system (super-fluid nuclei) [66], the ground to ground state Q values for neutron transfers is close to zero, matching the optimum Q -value (~ 0 MeV). It will be interesting to see how calculations including only transfer of $J = 0^+$ pairs to the 0_{gs}^+ states compare with the experimental data, improving our understanding of the origin of the enhancement factors.

In this context, it is also important to investigate the role played by neutron-proton correlations. These correlations are presently attracting peculiar interest in the field, especially making use of radioactive ion beams. As known, multinucleon transfer reactions allow the transfer of large number of nucleons, and in order to study proton-neutron correlation one has to use systems where the population of the $(\pm np)$ channels is allowed by the Q -value. First measurements of this kind have been very recently performed for $^{92}\text{Mo}+^{54}\text{Fe}$.

The problematic issue connected with the pair correlations is of current interest in ongoing research with radioactive beams, where for example the pairing interaction is expected to be significantly modified in nuclei with extended neutron distributions [68]. The recent works on ^{11}Li induced reactions [69] provided evidence of phonon mediated pairing interaction [70].

7 Conclusions

Significant advances have been made in the last years in the field of multinucleon transfer reactions. Via multiple transfers of neutrons and protons one could populate nuclei moderately far from stability, especially in the neutron-rich region, important for both reaction mechanism and nuclear structure. Valuable information on nucleon-nucleon correlations could be also derived, particularly in studies below the Coulomb barrier. Present focus is also in the study of the properties of the heavy binary partner, important for astrophysics. The presence of secondary effects, namely nucleon evaporation and transfer induced fission, need to be more carefully investigated, especially near the Pb and in the actinide regions, where other production methods, like fission or fragmentation, have severe limitations.

Acknowledgements

The material presented in this paper is the result of the work of many people which I would like to thank, in particular S. Szilner, T. Mijatović, N. Soić, D. Jelavić Malenica (RBI, Croatia), G. Pollarolo (TO, Italy), E. Fioretto, A. M. Stefanini, J. J. Valiente-Dobón (LNL, Italy), D. Montanari, G. Montagnoli, F. Scarlassara, E. Farnea, C. Michelagnoli, C. A. Ur (PD, Italy), A. Goasduff, F. Haas (Strasbourg, France) and the CLARA and Agata collaborations.

References

- [1] L. Corradi, G. Pollarolo and S. Szilner, *J. of Phys. G: Nucl. Part. Phys.* **36**, 113101 (2009)
- [2] A. M. Stefanini et al, *Nucl. Phys. A* **701**, 217c (2002)
- [3] S. Szilner et al, *Phys. Rev. C* **76**, 024604 (2007)
- [4] H. Savajols et al., *Nucl. Phys. A* **654**, 1027c (1999)
- [5] A. Cunsolo et al., *Nucl. Instr. and Meth. in Phys. Res. A* **481**, 48 (2002)
- [6] A. Gadea et al, *Eur. Phys. J. A* **20**, 193 (2004)
- [7] S. L. Shepherd et al, *Nucl. Instr. and Meth. in Phys. Res. A* **434**, 373 (1999)

- [8] A. Gadea et al., Nucl. Instr. and Meth. in Phys. Res. A **654**, 88 (2011)
- [9] <http://www.ganil.fr/research/developments/spiral2>
The Scientific Objectives of the Spiral2 Project (2006)
- [10] SPES: (<http://web.infn.it/spes/>) *Exotic beams for science*
- [11] L. Corradi et al., EMIS2012, Matsue (Japan), Dec. 3-7, 2012, to be published in Nucl. Instr. and Meth. B
- [12] S. Szilner et al, Phys. Rev. C **71**, 044610 (2005)
- [13] R. A. Broglia and A. Winther *Heavy Ion Reactions* (Addison-Wesley Pub. Co., Redwood City CA, 1991)
- [14] L. Corradi et al, Phys. Rev. C **66**, 024606 (2002)
- [15] L. Corradi et al, Phys. Rev. C **59**, 261 (1999)
- [16] C. H. Dasso, G. Pollarolo and A. Winther, Phys. Rev. Lett. **73**, 1907 (1994)
- [17] D. Montanari et al., Eur. Phys. J. A **47**, 4 (2011)
- [18] T. Mijatović et al., *Nuclear Structure and Dynamics 2012*, edited by T. Nikšić et al., AIP Conf. Proc. 1491, 346 (2012)
- [19] A. Winther, program GRAZING, <http://www.to.infn.it/~nanni/grazing>
- [20] A. Winther, Nucl. Phys. A **572**, 191 (1994)
- [21] A. Winther, Nucl. Phys. A **594**, 203 (1995)
- [22] D. Montanari et al, Phys. Rev. C **84**, 054613 (2011)
- [23] L. Corradi, Nucl. Phys. A **834**, 129c (2010)
- [24] G. Pollarolo and A. Winther, Phys. Rev. C **62**, 054611 (2000)
- [25] G. Pollarolo, Phys. Rev. Lett. **100**, 252701 (2008)
- [26] V. Zagrebaev and W. Greiner, Phys. Rev. Lett. **101**, 122701 (2008)
- [27] G.G. Adamian, N.V. Antonenko and D. Lacroix, Phys. Rev. C **82**, 064611 (2010)
- [28] M. Grasso, D. Lacroix and A. Vitturi, Phys. Rev. C **85**, 034317 (2012)
- [29] C. Simenel, Phys. Rev. Lett. **105**, 192701 (2010)
- [30] C. Simenel, Phys. Rev. Lett. **106**, 112502 (2011)
- [31] M. Evers et al., Phys. Rev. C **84**, 054614 (2011)
- [32] B. Yilmaz et al, Phys. Rev. C **83**, 064615 (2011)
- [33] G. Scamps and D. Lacroix, Phys. Rev. C **87**, 014605 (2013)
- [34] K. Sezikawa and K. Yabana,
<http://arxiv.org/abs/1303.0552>
- [35] S. Lunardi et al, Phys. Rev. C **76**, 034303 (2007)
- [36] B. Fornal et al., Phys. Rev. C **77**, 014304 (2008)
- [37] P. -A. Söderström et al., Phys. Rev. C **81**, 034310 (2010)
- [38] Z. M. Wang et al., Phys. Rev. C **81**, 054305 (2010)
- [39] S. Bottoni et al., Phys. Rev. C **85**, 064621 (2012)
- [40] S. Bhattacharyya et al., Phys. Rev. Lett. **101**, 032501 (2008)
- [41] S. Bhattacharyya et al., Phys. Rev. C **79**, 014313 (2009)
- [42] J. Ljungvall et al., Phys. Rev. C **81**, 061301(R) (2010)
- [43] A. Dijon et al., Phys. Rev. C **83**, 064321 (2011)
- [44] B. Fernandez-Dominguez et al., Phys. Rev. C **84**, 011301(R) (2011)
- [45] S. M. Brown et al., Phys. Rev. C **85**, 011302(R) (2012)
- [46] J. J. Valiente-Dobon et al, Phys. Rev. Lett. **102**, 242502 (2009)
- [47] D. Mengoni et al., Phys. Rev. C **82**, 02430 (2010)
- [48] S. Szilner et al, Phys. Rev. C **84**, 014325 (2011)
- [49] F. Recchia et al, Phys. Rev. C **85**, 064305 (2012)
- [50] S. Szilner et al., Phys. Rev. C, **87**, 054322 (2013)
- [51] D. Montanari et al, Phys. Lett. B **697**, 288 (2011)
- [52] D. Montanari et al, Phys. Rev. C **85**, 044301 (2012)
- [53] K.-L. Kratz et al., Astrophys. J. **403**, 216 (1994)
- [54] H. Grawe et al., Rep. Prog. Phys. **70**, 1525 (2007)
- [55] Y. Watanabe et al., EMIS2012, Matsue (Japan), Dec. 3-7, 2012, to be published in Nucl. Instr. and Meth. B
- [56] S. C. Jeong, *Construction proposal for KEK Isotope Separation System for β -decay spectroscopy*, RIBF NP-PAC-06, 2009.
- [57] C. L. Jiang et al., Phys. Rev. C **57**, 2393 (1998)
- [58] L. Corradi et al, Phys. Rev. C **84**, 034603 (2011)
- [59] N. Marginean et al, Phys. Rev. C **80**, 021301(R) (2009)
- [60] A. Shrivastava et al., Phys. Rev. C **80**, 051305R (2009)
- [61] V.I. Zagrebaev and W. Greiner, Phys. Rev. C **87**, 034608 (2013)
- [62] B. F. Bayman and J. Chen, Phys. Rev. C **26**, 1509 (1982)
- [63] E. Maglione et al, G. Pollarolo, A. Vitturi, R. A. Broglia and A. Winther, Phys. Lett. B **162**, 59 (1985)
- [64] J. H. Sorensen and A. Winther, Nucl. Phys. A **550**, 306 (1992)
- [65] W. von Oertzen et al., Eur. Phys. J. A **20**, 153 (2004)
- [66] D. Montanari et al., *NN2012*, S. Antonio, Texas (USA) May 27 - June 1, 2012, to be published in J. of Phys. G.
- [67] S. Szilner et al, Eur. Phys. J. A **21**, 87 (2004)
- [68] J. Dobaczewski, I. Hamamoto, W. Nazarewicz, and J. A. Sheikh, Phys. Rev. Lett. **72**, 981 (1994)
- [69] I. Tanihata et al, Phys. Rev. Lett. **100**, 192502 (2008)
- [70] G. Potel, F. Barranco, E. Vigezzi and R. A. Broglia, Phys. Rev. Lett. **105**, 172502 (2010)